FERMILAB-CONF-17-216-E
ACCEPTED

The Muon $g-2$ experiment at Fermilab

James Mott[1]

Boston University, Boston, MA 02215, U.S.A

Abstract

The Muon $g-2$ experiment at Fermilab will measure the anomalous magnetic moment of the muon to a precision of 140 ppb, reducing the experimental uncertainty by a factor of 4 compared to the previous measurement at BNL (E821). The measurement technique adopts the storage ring concept used for E821, with magic-momentum muons stored in a highly uniform 1.45 T magnetic dipole field. The spin precession frequency is extracted from an analysis of the modulation of the rate of higher-energy positrons from muon decays, detected by 24 calorimeters and 3 straw tracking detectors. Compared to the E821 experiment, muon beam preparation, storage ring internal hardware, field measuring equipment, and detector and electronics systems are all new or significantly upgraded. Herein, I report on the status of the experiment as of Sept. 2016, presenting the magnetic field uniformity results after the completion of the first round of shimming and outlining the construction progress of the main detector systems.

1. Introduction

The anomalous magnetic moment of the muon, $a_\mu \equiv (g_\mu - 2)/2$, is a quantity of particular interest because it can be both measured and predicted to a high level of accuracy. For spin-½ particles, a_μ is 0, but higher-order effects from virtual loops cause the value to increase. A comparison ofan experimental measurement and theoretical prediction therefore enables stringent tests for the presence of new physics, which could cause a disparity due to effects from non-SM particle loops. The current predictions of contributions to a_μ are presented in Table 1.

The contributions break down into four main components: QED, hadronic vacuum polarization (HVP), hadronic light-by-light (HLbL) and electroweak. The QED component is by far the largest contributor, but due to hugely impressive calculations, it is known to five-loop level and has the smallest associated uncertainty. The contributions from the hadronic sector dominate the total uncertainty (a total of 43 ppm compared to 0.01 ppm for QED and electroweak combined). There is a great deal of work being undertaken by the theory community to constrain and reduce the uncertainty on these contributions, with at least 12 presentations on the subject at this workshop alone. The HVP contribution is determined from experiment through a dispersion relation and the measurement of the $e^+e \to$ hadrons cross section. Its uncertainty currently dominates the total SM uncertainty, but this is expected to reduce by a factor of two on the timescale of this experiment as a result of on-going experimental campaigns at BESIII and VEPP-2000, along with continued analysis of the BaBar data set. The HLbL contribution originates from model-dependent calculations and its uncertainty cur-

a_μ Contribution	Value ($\times 10^{-11}$)
QED (γ & $l^\pm$) [1]	116 584 718.951 ± 0.08
Hadronic VP (lo) [2]	6923 ± 42
Hadronic VP (ho) [3]	−98.4 ± 0.7
Hadronic LbL [4]	105 ± 26
Electroweak [5]	153.6 ± 1.0
Total SM	116 591 802 ± 49

Table 1: Current estimates for SM contributions to a_μ.

Email address: jmott@bu.edu (James Mott)

[1] On behalf of the Muon $g-2$ experiment

rently depends on assessments of the various strengths and limitations of different hadronic models. More recently, there have been significant advances in lattice QCD predictions of both hadronic contributions and an uncertainty goal of 10% for HLbL within the timescale of the experiment seems acheivable.

Currently the best experimental measurement of a_μ comes from this experiment's predecessor: the BNL E821 experiment. The final result of $a_\mu = 116\,592\,089\,(54)_{st}\,(33)_{sy}\,(63)_{tot} \times 10^{-11}$ [6, 7] leads to a discrepancy between experiment and theory at the level of $\Delta a_\mu = [287 \pm 80] \times 10^{11}$ or 3.6σ. This intriguing difference provides the motivation for the Muon $g-2$ experiment at Fermilab (E989), which will measure a_μ with 21 times higher statistics and a reduction in systematic uncertainty by a factor $2-3$ compared to the BNL experiment. If the central values remain unchanged, then the combined reduction in experimental and theoretical uncertainties would lead to a discrepancy at the level of 7.5σ (or 5σ with only experimental improvements).

2. Muon $g-2$ experiment at Fermilab

The Muon $g-2$ experiment at Fermilab [7] follows the same experimental principle as the BNL E821 experiment. Longitudinally-polarised muons are injected into a storage ring with a near uniform magnetic dipole field. The anomalous magnetic moment, a_μ, is extracted by measuring the magnetic field averaged over the muon distribution, B, and the anomalous precession frequency, ω_a. These are related by

$$\omega_a = \omega_s - \omega_c = \frac{e}{mc}\left[a_\mu B - \left(a_\mu - \frac{1}{\gamma^2-1}\right)(\beta \times E)\right], \quad (1)$$

where ω_s is the spin precession frequency of the muons in the magnetic field and ω_c is their cyclotron frequency. The second term is a result of the boost of electric fields present in the laboratory to the muon rest frame and vanishes for muons stored at the "magic momentum" of 3.09 GeV. In reality, stored muons have a small momentum spread resulting in a correction to the measured precession frequency.

Modification of the accelerator at Fermilab to provide a high-purity (π fraction $< 10^{-5}$), intense (8×10^6 μ^+/sec) beam of $\sim$ 96% longitudinally-polarised μ^+ is 75% complete. 8 GeV protons from the booster will be fired at the former Tevatron anti-proton production target and outgoing π^+ are focussed by a lithium lens with momentum selection centred on 3.11 GeV. These pions are transported along a 270 m beamline and directed into a delivery ring, where they are stored in order to allow for more decay time and for separation of any proton contamination. After several turns, the muons are kicked from the delivery ring into a final beamline that terminates at the storage ring entrance.

The storage ring from the BNL E821 experiment will be reused in E989. Muons are injected into the ring through a superconducting inflector magnet that nullifies the magnetic field of the storage ring. At the exit of the inflector, the muons are on a non-central orbit. This is corrected during the first turn around the ring when a fast magnetic kicker applies an 11 mrad kick. The captured beam will have a small, but non-zero, transverse momentum such that vertical containment is required. Four electrostatic quadrupoles operating at 32 kV serve this purpose, creating a Penning trap in which the muons undergo cyclotron motion with a period of 149 ns.

Once the muons are successfully stored in the ring, calorimeters placed in the interior are used to measure ω_a via the modulation of high-energy positrons from muon decay (Section 4). Simultaneously, the magnetic field is measured using pulsed proton NMR (Section 3). In addition to the main goal of the experiment, a search will also be undertaken for an electric dipole moment (EDM) of the muon with an improved sensitivity of two orders of magnitude to 10^{-21} e·cm.

Following a high profile move of the superconducting coils from BNL, the storage ring was reassembled in a newly constructed building in the "Muon Campus" of Fermilab. Full field strength was reached in Sept. 2015, allowing for the start of a long process of improving field uniformity with field shimming.

3. Magnetic Field

The magnet for the experiment is the same one that was used in the E821 experiment. It is a 14 m diameter toroidal C-shaped magnet, made up of 12 iron yokes and superconducting coils, carrying a current of 5.2 kA to provide a 1.45 T dipole magnetic field.

A measurement of the magnetic field strength is one of two ingredients that determine the value of a_μ. To achieve the required sensitivity, pulsed proton NMR is used with 400 fixed probes located above and below the muon storage volume. Interpolation between these is cross-checked with a trolley containing 17 NMR probes that rides on a set of rails inside the vacuum chamber and measures the field exactly at the muon storage location. The absolute field probe from E821 is also being re-used to translate from the proton Larmor precession frequencies to an absolute magnetic field value. This was also the same probe used in the muonium hyperfine experiment from which the muon-to-proton magnetic

moment ratio is drawn [8], reducing another source of potential systematic uncertainty. Further to this, new absolute probes are also under development.

The particular quantity of interest for extracting a_μ is the magnetic field averaged over the muon distribution. To reduce the required precision of our knowledge of the muon distribution and to reduce other key systematics, the magnetic field is made as uniform as possible. The target levels are ±25 ppm for point-to-point variations and <1 ppm when averaged azimuthally around the ring.

The magnet has many calibration tools that can be used to improve the uniformity of the ring, as shown in Figure 1. Placement of different magnetic components affects the field strength and direction in local regions. 72 high-purity iron pole pieces and 48 iron top hats are used to make coarse changes to the dipole field and 864 iron wedges and 144 edge shims are deployed to reduce any quadrupole or sextupole asymmetries. On a sub-degree level, 8000 thin iron foils are stuck to the surface of the poles to provide very localised modifications. Finally, 100 active surface coils with controllable currents remove ring-wide average field moments.

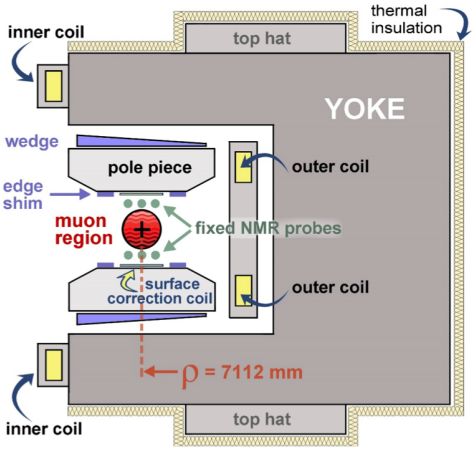

Figure 1: Cross-section through the $g-2$ magnet. Muons travel around the ring, out of the page.

The passive shimming pieces are intended to account for very small (<100 μm) placement errors and intrinsic magnetic material variances. OPERA simulations of the field were calibrated against large shim movements, allowing for the calculation of desired shim positions to increase the field uniformity. Calibration of the passive shimming tools began in Oct. 2015 and an iterative shimming procedure was completed in Aug. 2016. The field uniformity at the start and end of this process can be seen in Figure 2. At the starting point, the variation in the field was at the level of 1400 ppm with a visible repeating structure from slightly misaligned pole pieces. After the shimming process, the field is much more uniform, lying within the ±25 ppm point-to-point variation goal.

The uncertainty on a_μ resulting from the field measurement is wholly systematic. The target improvement is from 170 ppb at E821 to 70 pbb with this experiment. Most of the individual systematics can be reduced to an acceptable level by small improvements rather than drastic changes. These small improvements include better knowledge of the NMR trolley location, reduced trolley temperature changes, a greater degree of temperature control in the experimental hall, an enlarged set of viable fixed NMR probes, and storage of the full probe waveforms to enable measurements in regions of higher field gradients.

4. Detector Systems

The detector systems for the experiment are entirely new and comprise 24 calorimeters for determining the arrival time and energy of decay positrons and three straw trackers for measuring positron tracks that can be extrapolated back to infer the point of muon decay. In addition, sets of scintillating fibre hodoscopes are used to measure the stored muons' xy profile and to determine the incoming beam parameters.

A measurement of ω_a is the second key part of the measurement of a_μ. The spin precession frequency is observable due to parity violation in $\mu^+ \rightarrow e^+ \bar{\nu}_\mu \nu_e$ decay. The highest energy positrons are preferentially emitted when their momentum is aligned with the muon spin, so the spin direction can be inferred from calorimeter measurements of decay times of positrons with an energy above a given threshold. Data from the E821 experiment showing the modulation of the decay rate by ω_a is displayed in Figure 3.

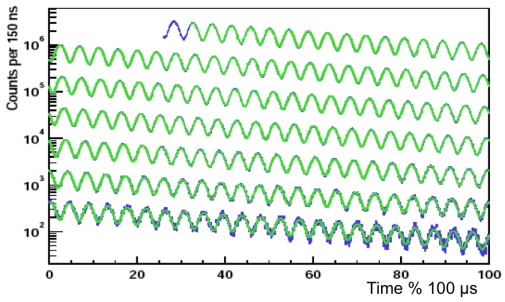

Figure 3: The number of positrons with $E > 1.8$ GeV as a function of time, from the E821 experiment [6]. The modulation is at the anomalous precession frequency.

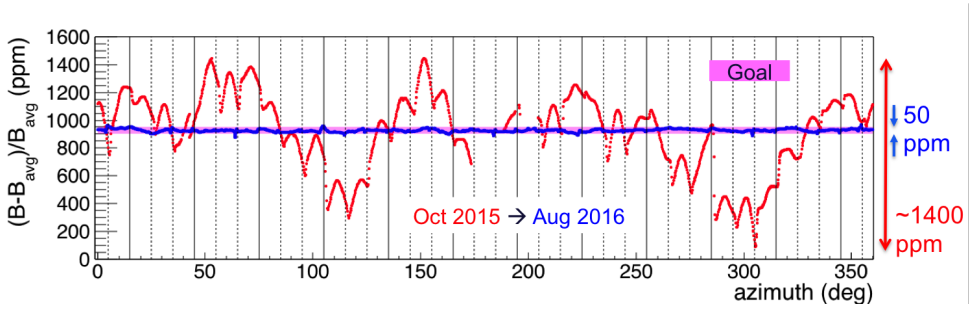

Figure 2: Magnetic field uniformity at initial switch-on of the magnet and after the final round of rough shimming, showing that the target uniformity has been met.

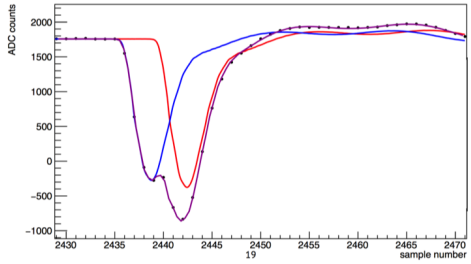

Figure 4: Two electrons, 5 ns apart, as measured by a $g-2$ calorimeter at SLAC in 2015.

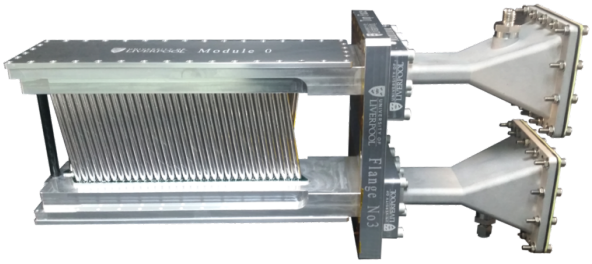

Figure 5: One tracker module housing 128 straws. Eight modules make up each of the three tracker stations.

24 calorimeters, each made up of an array of 6x9 PbF_2 crystals, will be deployed inside the ring to make this measurement. Each of the crystals is read out by a SiPM and the waveform is digitised at 800 MSPS with 12-bit resolution by custom frontend boards.

Pile-up is a significant source of systematic error, since two low-energy positrons striking a crystal at a similar time can be mistaken for a higher-energy positron. The pile-up rate changes as muons decay away and so these misidentifications are time-dependent and can directly impact the ω_a measurement. The segmentation of the calorimeter allows for spatial separation of positrons and the the fast response of the crystals as well as the high frequency digitisation of the waveform allow temporal separation down to the 5 ns level [9] (Fig. 4).

The intra-fill gain stability of the calorimeter is very important as the measurement relies on selecting positrons above a given threshold. In order to ensure stability, a dedicated laser calibration system has been developed which overlays laser pulses every 5 µs throughout a storage ring fill [10].

In front of three of the calorimeters are three tracker stations, each comprising eight modules for a total of 3000 straws (see figure 5). The main role of the trackers is to measure the beam profile of the stored muons, which is required to properly weight the magnetic field measurements as well as to quantify the largest corrections to the ω_a measurement. In addition, the trackers will be used to cross-calibrate the calorimeter, check pile-up identification techniques and track muons lost from the storage region.

This work was supported in part by the US DOE.

[1] T. Aoyama, et al., Complete Tenth-Order QED Contribution to the Muon g-2, Phys. Rev. Lett. 109 (2012) 111808.
[2] M. Davier, et al., Reevaluation of the Hadronic Contributions to the Muon g-2 and to $\alpha(M_Z)$, Eur. Phys. J. C71 (2011) 1515.
[3] K. Hagiwara, et al., $(g-2)_\mu$ and $\alpha(M_Z^2)$ re-evaluated using new precise data, J. Phys. G38 (2011) 085003.
[4] J. Prades, et al., The Hadronic Light-by-Light Scattering Contribution to the Muon and Electron Anomalous Magnetic Moments, Adv. Ser. Dir. HEP 20 (2009) 303–317.
[5] C. Gnendiger, et al., The electroweak contributions to $(g-2)_\mu$ after the Higgs boson mass measurement, Phys. Rev. D88.
[6] G. W. Bennett, et al., Final Report of the Muon E821 Anomalous Magnetic Moment Measurement at BNL, Phys. Rev. D73 (2006) 072003.
[7] J. Grange, et al., Muon (g-2) Technical Design Report, arXiv:1501.06858 [physics.ins-det].
[8] W. Liu, et al., High precision measurements of the ground state hyperfine structure interval of muonium and of the muon magnetic moment, Phys. Rev. Lett. 82 (1999) 711–714.
[9] A. T. Fienberg, et al., Studies of an array of PbF_2 Cherenkov crystals with large-area SiPM readout, Nucl. Instrum. Meth. A783 (2015) 12–21.
[10] A. Anastasi, et al., Test of candidate light distributors for the muon (g-2) laser calibration system, Nucl. Instrum. Meth. A788 (2015) 43–48.